

Hydride Embrittlement Analysis on the End Cap Welded Zone and Heat Affected Zone of Zr-Nb alloy tube

Sangbum Kim, Youho Lee*

Seoul National University, 1 Gwanak-ro, Gwanak-gu, Seoul 08826, Republic of Korea

*Corresponding author: : leeyouho@snu.co.kr

1. Introduction

Nuclear fuel cladding tube to end cap welding is a process of loading UO₂ pellet into the Zircaloy cladding tube, bringing the cladding tube and end cap into contact, and welding them in the circumferential direction to seal. The welded area of nuclear fuel rods has high possibility of leakage during the operation. In order to prevent leakage of fissile material during the operation in a nuclear reactor, high integrity of a welding quality is required. Extensive studies have been done on the integrity of welding and optimal welding options. Nevertheless, in terms of spent nuclear fuel (SNF) management, little attention has been given to the hydride embrittlement of the cladding welded area.

Welding produces residual stresses and local changes in microstructure and crystallographic texture [1]. As the microstructure of the welded area changes with the welding process, the mechanical properties of the weld differ from those of the unwelded area of the tube. Also, since hydride formation and interconnectivity vary depending on the grain size and microstructure of the material [2], it can be expected that the hydride embrittlement of the welded area might be different from that of the unwelded tube region.

Therefore, as an effort to provide base experimental data for hydride embrittlement of cladding welded area in SNF, this study investigates hydride embrittlement analysis on the welded zone (WZ) and heat affected zone (HAZ) of Zr-Nb alloy tube. This paper will provide a basic understanding of the hydride embrittlement on the welded area, and give an opportunity to reexamine the welded area structural integrity in terms of SNF management.

2. Methodology

2.1 Material

In the following test, cold work stress-relief annealed (CWSR) Zr-Nb alloy with an outside diameter of 9.5 mm (9.55 ~ 9.65 mm at welded area) and a wall thickness of 0.57 mm were used. As depicted in Fig. 1(a), the experimental specimens were used from the reactor grade as-received tubular cladding with end cap welded. The chemical composition of the material is presented in Table. 1.

The cladding tube to end cap welding is done by KEPCO NF using a resistance upset butt welding method. Resistance upset butt welding method welds with a current of 12 ~ 14.0 kA in a very short time of 1/20 ~

1/60 second [3]. The local temperature of weld zone (WZ) rises above the zirconium melting point (1855 °C) [4], but the heating and cooling rate are very fast (~ 10³ °C/sec). Thus, the grain growth in WZ is minimized and the heat-affected zone (HAZ) gets smaller [5].

Table. 1. Chemical composition of Zr-Nb alloy (mass %)

Element	Sn	Fe	Cr	O	Zr	Nb
Zr-Nb alloy	0 ~ 0.99	0.11	-	0.11	bal.	0.98

2.2 Experiment Setup

In this study, the optical microscope observation and Field Emission Scanning Electron Microscopy (FE-SEM) analysis is done for microstructure characterization. Hydrogen is charged into cladding to apply burnup effects. The end cap welded fuel rod tube was cut to 6 cm length and placed in a vacuum furnace. Hydrogen charging was performed at 400 °C. After 24 h of heat treatment, specimens are slowly cooled down to room temperature at a cooling rate of 0.5 °C/min. Hydrogen content was determined from the hydrogen determinator (ONH-2000). Subsequently, as depicted in Fig. 1(b), the hydrogen-charged and as-received specimens were cut to a 5 mm length for the ring compression test (RCT).

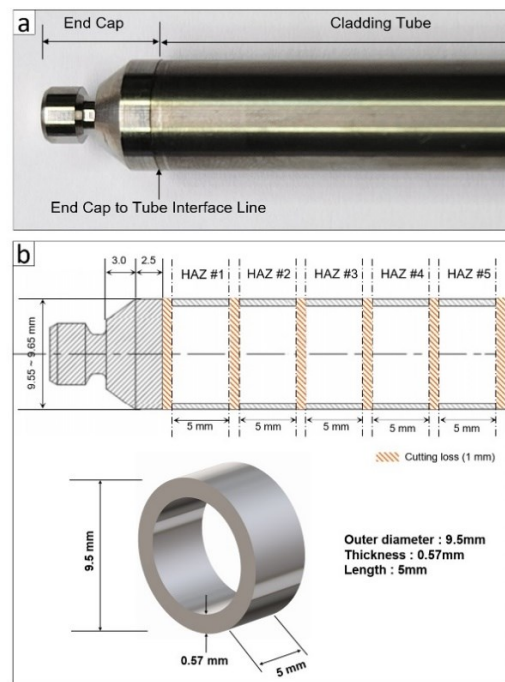


Fig. 1. (a) Tube to End Cap Interface of Zr-Nb alloy and (b) the specimen dimensions for RCT

RCTs were conducted with the slow rate of 0.033mm/sec to obtain load (stress) - strain curves for the specimens. Hardness at weld interface was examined by Vickers micro hardness testing machine (HM-210).

3. Results and Discussion

3.1 Microstructure characterization

The transverse section of the as-received specimen was cut to find for microstructure observation. However, it was difficult to observe the microstructure of the welded area with SEM.

The microstructure can be roughly distinguished into end cap area, HAZ, WZ, and cladding tube regions through backscattered electron (BSE) imaging using FE-SEM. The end cap consisted of large, equiaxed grains in contrast to the cladding tube. The ratio of large equiaxed grains decreased from end cap to HAZ. It was difficult to ascertain whether the grains were recrystallized in the high-temperature environment expected in the WZ and HAZ. Although it is not possible to determine the texture with BSE, it seems that macro-textures and patterns of the cladding tube are formed in the axial direction due to the pilgering process, and the texture of WZ is significantly different from this.

Figure 3 shows the results observed with an optical microscope (OM) after polishing and etching the half cut of the specimen loaded with hydrogen. The averaged hydrogen concentration of this specimens is 815 wppm.

From the hydride image in Fig. 3(a), it can be seen that the microstructure of each region is different through the morphology of the hydride formation. Fig. 3(b) is a hydride image of the end cap area. As confirmed in the BSE image, this area is composed of equiaxed grains, so the density of grain boundaries is not high compared to other areas. Due to this, the connectivity of the hydrides is low, and it seems that the hydrides are formed in a random direction.

Fig. 3(c) shows that a very small amount of hydride was formed inside WZ. And hydrides clearly formed in the axial direction were seen on both sides of WZ, which is expected to be HAZ. The gap in the radial direction of the hydride in the HAZ part was wider than that of the cladding tube area in Fig. 3(d). As a result of analyzing the amounts of precipitated hydrides in the order of HAZ#1 to HAZ#5 (see Fig. 1 (b)), they were 410, 763, 812, 780, and 820 wppm, respectively. It was confirmed that the hydrogen concentration was relatively low in HAZ #1, which is closest to WZ. This relatively small amount of hydride precipitation is likely to have a significant impact on material strength.

Only a very rough classification of each region was possible with the microstructure analysis using BSE and OM, and it seems that EBSD or TEM should be used for more in-depth analysis.

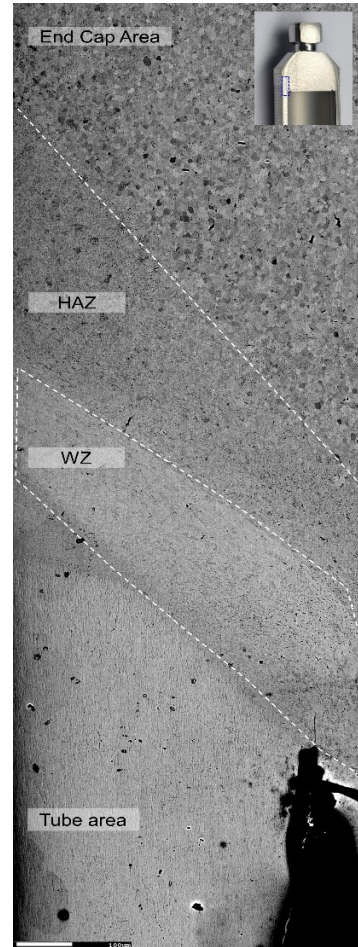


Fig. 2. BSE SEM Macrographs of welded area (End cap area, HAZ, WZ, and tube area are roughly distinguishable.)

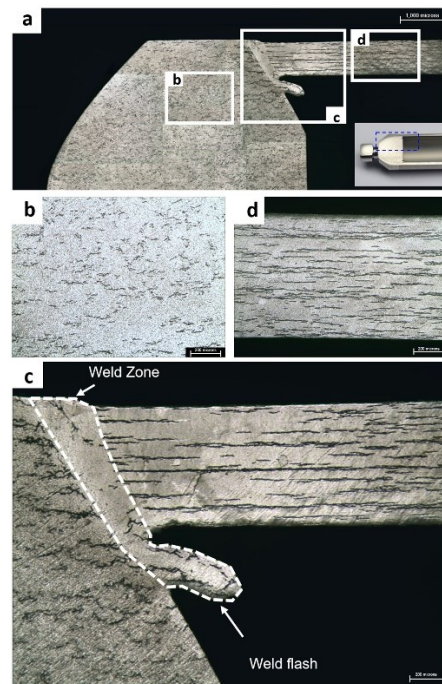


Fig. 3. OM image of Hydrided specimen (815 wppm), (a) Macrographs of welded area, (b) End cap area, (c) WZ and HAZ, (d) cladding tube area

3.2 Mechanical test (RCT) and Hardness test

The structural integrity of the welded area was confirmed through the load (stress)-strain curve obtained by RCT for each area. As shown in Fig. 2, WZ is not easy to perform specimen cutting and RCT because the axial length is only about 200 microns. Therefore, RCT evaluation was performed only for HAZ #1 to HAZ #5. The obtained curve is shown in Fig. 4.

Looking at the results for as received HAZs indicated by the solid line, HAZ#3, #4, and #5 separated from WZ have a fracture load of 0.57~0.59kN and a value of about 60% strain. On the other hand, the results of HAZ#1 and #2, which are close to WZ, show a fracture load of less than 0.53 kN and a strain of about 55%. It can be seen that HAZ#1 and #2 are heat affected zones, and mechanical properties are slightly degraded by welding, and the area more than 10mm away from WZ is not HAZ.

In the case of specimen with hydride, as shown in Fig. 3(c), HAZ#1 with the lowest hydrogen content showed the highest mechanical properties. In case of hydrided HAZ#5 with the highest hydrogen concentration, the fracture load is 0.42 kN and the strain is over 35%.

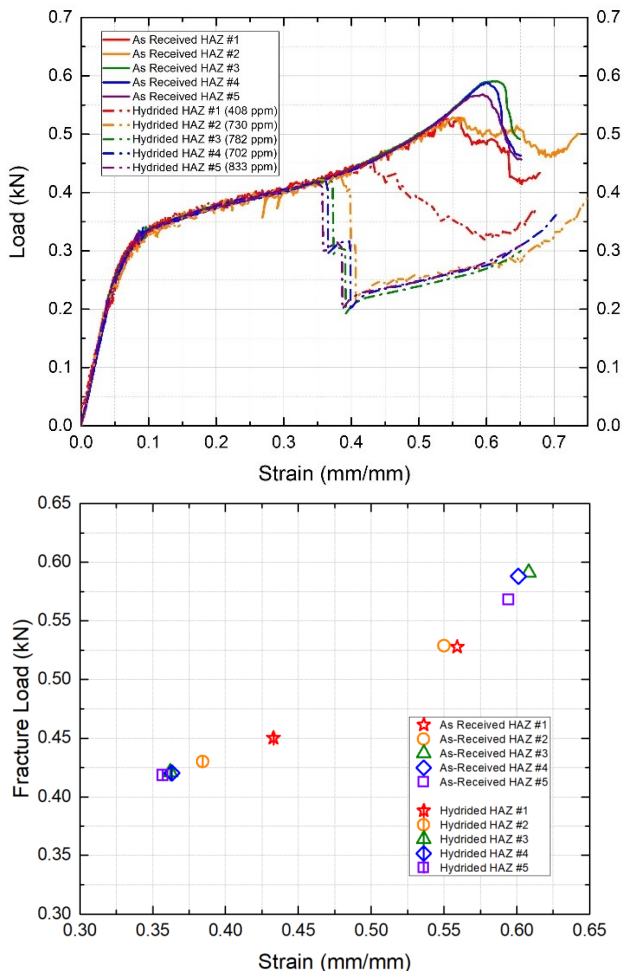


Fig. 4. Mechanical test result on the HAZ #1~#5, (up) load-strain curves, (down) Fracture load-strain scatter plot

Through the RCT experiment, it was confirmed that the area within 10 mm of WZ was the actual HAZ. Although the mechanical properties of the HAZ were lowered due to microstructural changes after welding, it was not at a level that threatened the material integrity. As less hydride is precipitated in HAZ by about half and less hydride is formed in WZ, WZ and HAZ have better mechanical properties in terms of hydride embrittlement.

As an additional experiment, the mechanical properties of each area were compared through Vickers hardness measurement in the axial direction from the end cap (Fig. 5). The load of the Vickers hardness tester was measured by pressing for 15 seconds with 0.3 kgf. The hardness values in the end cap area with large grain size were distributed around 180 ~ 200. And hardness slightly increased to about 200 ~ 210 in the upper HAZ part, and showed a high hardness value of 250 ~ 280 in WZ. This was higher than the tube hardness value of 235 ~ 240.

In general, since there is a proportional relationship between material hardness and tensile strength, the tensile strength of WZ is expected to be higher than that of the tube region. In addition, the thickness of the cladding tube is 0.57mm, whereas the thickness of the weld flash formed in WZ is about 0.45mm, so the load-bearing cross-sectional area is large. Therefore, when sound welding is performed without welding defects, it is analyzed that the material integrity of WZ is superior to that of the tube area.

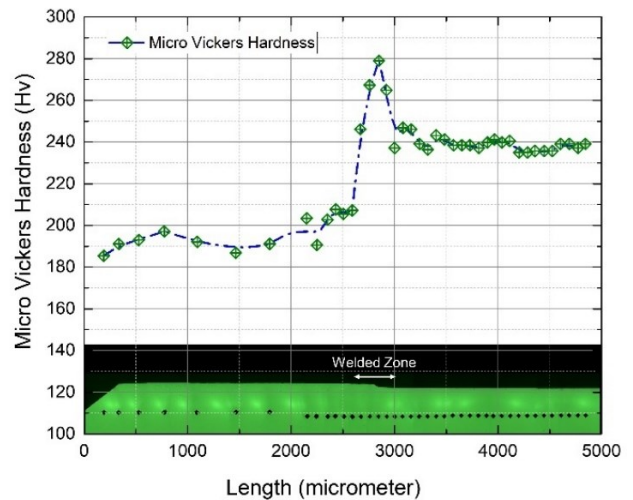


Fig. 5. Micro Vickers Hardness Result of As-Received Specimen

4. Conclusions

This study presents the hydride embrittlement of Zr-Nb alloy on the end cap welding area, and discusses the microstructure on the WZ and HAZ. Key findings and implications of this study are as follows.

1. In the end cap to tube welding, the area within 10 mm of WZ can be considered as HAZ.

2. Microstructural analysis through OM, and SEM have a limitation. Further microstructural analysis can be initiated via EBSD analysis.
3. The strength and strain of the HAZ is lowered due to microstructural changes after welding, however, it is not at a level that threatened the material integrity.
4. On the contrary, WZ and HAZ have better mechanical properties than the tube area in terms of hydride embrittlement due to less hydrides area precipitated.
5. Hardness of WZ is the highest among other area in the fuel rod.

ACKNOWLEDGEMENT

This work was supported by the Institute for Korea Spent Nuclear Fuel (IKSNF) and National Research Foundation of Korea (NRF) grant funded by the Korea government (Ministry of Science and ICT, MSIT) (2021M2E1A1085226).

REFERENCES

- [1] C. E. Coleman, G. L. Doubt, R. W. Fong, J. H. Root, J. W. Bowden, S. Sagat, and R. T. Webster, Mitigation of harmful effects of welds in zirconium alloy components, Zirconium in the Nuclear Industry: Tenth International Symposium, ASTM International, 1994.
- [2] W. Qin, J. A. Szpunar, N. K. Kumar and J. Kozinski, Microstructural criteria for abrupt ductile-to-brittle transition induced by δ -hydrides in zirconium alloys, *Acta materialia*, Vol. 81, pp. 219-229, 2014.
- [3] T. H. Na, S. J. Na, and Y. W. Park, A study on characteristics of end plug resistance welding process in nuclear fuel rods by experiment and numerical simulation, *The International Journal of Advanced Manufacturing Technology*, Vol. 98.9, pp. 2241-2255, 2018.
- [4] A. M. Rizzo, M. V. Alvarez, J. R. Santisteban, P. Vizcaino, S. Limandri, M. R. Daymond, and S.C. Vogel, Crystallographic texture and microstructural changes in fusion welds of recrystallized Zry-4 rolled plates. *Journal of Nuclear Materials*, 488, 83-99. 2017.
- [5] S. S. Kim, J. H. Koh, J. W. Lee, and G. I. Park, Application of Welding Technology for a Zirconium Alloy of Nuclear Fuel Cladding, *Journal of Welding and Joining*, Vol. 29(1), pp. 5-8. 2011.